Molecular dynamics simulation of disorder-induced heating in ultracold neutral plasma

L. Guo, R. H. Lu,* and S. S. Han†

Key Laboratory for Quantum Optics and Center for Cold Atom Physics, Shanghai Institute of Optics and Fine Mechanics, Chinese Academy of Sciences, Shanghai 201800, China

(Received 20 October 2009; published 30 April 2010)

Disorder-induced heating (DIH) is one of the main reasons reducing the coupling strength in ultracold plasma. We propose applying an optical lattice as periodic confinement before the ultracold atomic cloud is ionized to eliminate its effect. We demonstrate a numerical simulation for the dynamics of the ultracold plasmas using classical molecular dynamics method with open boundary. DIH is reproduced in the simulation with the random Gaussian initial distribution and is absent in the results with the ordered lattice initial distribution. We further find that the collisional heating from electrons is important for ultracold plasmas with chosen spatial correlations in the optical lattice. Carefully preparing the initial condition (e.g., the ion density, initial electron temperature, and so on), collisional heating for the ions would be significantly reduced and eventually negligible. This allows a much stronger coupling in ultracold plasma to be realized.

DOI: 10.1103/PhysRevE.81.046406 PACS number(s): 52.27.Gr, 52.20.−j, 52.27.Cm, 52.27.Aj

I. INTRODUCTION

Recent experiments have produced ultracold plasmas from a laser-cooled atomic cloud confined in a magneto-optical trap [1–5]. By tuning the frequency of the ionizing laser, the initial energy of electrons E_e could be manipulated. These experiments pave the way toward an unexplored field of ultracold ionized gases and allow the discoveries of a series of new phenomena in atomic physics as well as in plasma physics.

One of the motivations of studying ultracold plasmas is the fact that the ultracold plasma is a strongly coupled system. The correlation strength is determined by the Coulomb coupling parameter $\Gamma = Z^2/(4\pi\varepsilon_0 a k_B T)$ (Z is the charge) with the Wigner-Seitz radius $a=[3/(4\pi\rho)]^{1/3}$ [6,7], where ρ is the plasma density. With this definition the plasma is strongly coupled if $\Gamma \gg 1$. A system is strongly coupled if it meets one of the following conditions: (a) high density, which leads to a large Coulomb potential; (b) low temperature, which leads to small thermal energy; and (c) highly charged states such as "dusty" plasmas. High density can be found in fusion plasma. However, the fusion plasma is hard to control and diagnose. The ultracold neutral plasma makes the low-temperature scenario to become possible. After the creation of ultracold neutral plasma, the ion kinetic energy could be as low as 10 μK, so the ions were strongly coupled, $\Gamma > 1000$ [1]. This also allows us to investigate the property of fusion plasma from the ultracold plasma experiments, which is easier to obtain and control in a laboratory condition.

The ultracold atomic cloud interacts weakly until the plasma is created. Once the plasma is formed it starts with a completely nonequilibrium state left by the original distribution of the atomic cloud. The conversion of Coulomb potential to kinetic energy rapidly heats the electrons and ions. This effect has been termed as "disorder-induced heating" (DIH) [8] or "correlation-induced heating" [9]. It shows that in a nonequilibrium state the potential energy is higher than that in an equilibrium state with the same average density. With the evolution of that ionized ultracold cloud, this heating effect would significantly reduce the coupling in the plasma and eventually lose their characters as a strong coupling system.

To maintain the strongly coupled condition, there are several suggestions to reduce the disorder heating effect [8,10,11]. However, it is harder to be realized experimentally. There is also a proposal about eliminating DIH by using optical lattices to apply periodic confinement to the neutral atoms [12] before the plasma is created. In this paper, we simulate the DIH effect in the ultracold plasma created by photoionizing neutral atoms with different initial conditions. We apply the classical molecular dynamics simulation with open boundary conditions with a N^2 scaling of all pairwise calculations. We shall discuss the possibility of using an optical lattice as a confining periodic potential to realize a crystal-like initial condition. By carefully selecting the initial parameters, we would show that the strong coupling property is maintained while the plasma is evolving.

II. THEORY

We use the classical molecular dynamics method to simulate the dynamics of the ultracold plasma. In order to simulate the strongly coupled plasma, the Coulomb interaction is calculated pairwisely for all the particles. This would avoid the inaccuracy coming from the truncation calculation. With our computing capability, it is possible to simulate the ultracold plasma with the Coulomb force calculated by this method when the particle number is finite.

The equations for the motion of charged particles are given by

$$\mathbf{r}_j(t+\tau) = \mathbf{r}_j(t) + \mathbf{v}_j(t)\tau + \frac{1}{2m_{i,e}}\mathbf{F}_j(t)\tau^2,$$

*lurh@mail.siom.ac.cn
†sshan@mail.shcnc.ac.cn

 ©2010 The American Physical Society

$$\mathbf{v}_j(t+\tau) = \mathbf{v}_j(t) + \frac{\tau}{2m_{i,e}}[\mathbf{F}_j(t) + \mathbf{F}_j(t+\tau)], \tag{1}$$

where τ is the simulation time step, $m_{i,e}$ is the mass of the ions (electrons), and $\mathbf{F}_j(t)$ describes the Coulomb force on particle j given by all other particles at time t, which depends on their relative coordinates.

To avoid singularities, the Coulomb potential is rounded to the form

$$1/\sqrt{|\mathbf{r}_1 - \mathbf{r}_2|^2 + \varepsilon^2}, \tag{2}$$

where $\varepsilon \ll a$ is the Wigner-Seitz radius. In the simulation we use the value of ε equal to $a/100$. It is small enough that the rounded Coulomb potential is a good approximation. We compare two simulating results for $\varepsilon = a/100$ and $\varepsilon = a/200$ and find that there is no observable difference on the scale we discuss. A further decrease in the value of ε does not change the collective behavior of particles in the plasma such as the temperature and density evolution. In this paper, the mass ratio is chosen to be $m_i/m_e = 100$ [13,14]. We choose this relatively low value, so that the ions spend less time to participate the correlation dynamics during the simulation. This relative low mass ratio would also cause faster electron-ion heating [13,15], but would not affect the DIH mechanism we shall discuss here.

The temperature is obtained from the molecular kinetic energy,

$$T = \frac{m}{3Nk_B}\sum_j^N \mathbf{v}_j'^2(t), \tag{3}$$

where N is the particle number and $\mathbf{v}_j'$ is the particle j velocity. For unconfined plasma expanding in the vacuum, the ion velocity would increase in the radial direction. An average ion acceleration for the Gaussian density profile is given by [17]

$$\dot{\mathbf{u}} = -\frac{k_B(T_e + T_i)}{m_i\rho_i}\nabla\rho_i = \frac{k_B(T_e + T_i)}{m_i\sigma^2}\mathbf{r}. \tag{4}$$

In the central region of the plasma, the distribution of the thermal velocity is close to the Maxwell-Boltzmann distribution, and the average kinetic energy is directly related to the ion temperature T. The kinetic energy becomes more and more dominated by radial expansion energy toward the edge of the plasma. We calculate the average ion kinetic energy from the velocity distribution in the inner region which is a spherical volume with the radius of $0.8R_0$ (R_0 denotes the initial plasma radius). Furthermore, our results show that, for fast expanding conditions, there is still a large radial expansion velocity included in the kinetic energy in the inner region. Because the radial expansion velocity is indistinguishable from the radial thermal velocity, an average of the radial velocity would not give us enough information about the particle temperature. We shall calculate average thermal velocity of the tangential direction to obtain the temperature T as

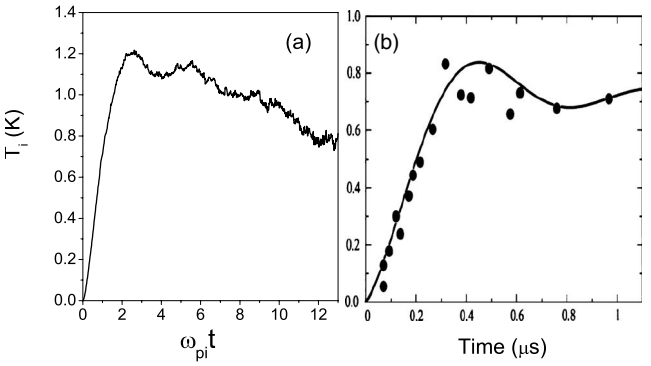

FIG. 1. The time evolution of the average kinetic energy of ions with random Gaussian initial distribution of the atoms: (a) the results from our simulation for low initial temperature $T_e(0) = 10$ K, $T_i(0) \sim 0$ K, $N_i = N_e = 7920$ and (b) the results obtained by a hybrid-MD calculation with initial peak density $\rho_0(0) = 2 \times 10^9$ cm^{-3} and electron temperature $T_e(0) = 38$ K. The results of a hybrid-MD calculation (solid line) are compared to experimental data (dots) [17,19].

$$Nk_BT = \frac{1}{2}m\sum_j^N (v_{j_\theta}^2 + v_{j_\varphi}^2). \tag{5}$$

Here, v_{j_θ} and v_{j_φ} are the thermal velocities in the directions of $\hat{\theta}$ and $\hat{\varphi}$, respectively.

III. SIMULATION RESULTS AND DISCUSSION

A. DIH for random Gaussian initial distribution of atoms

With the random Gaussian initial distribution of the ions, two conditions are compared. The first condition is that the initial temperatures of both electrons and ions are relatively low [$T_e(0) = 10$ K, $T_i(0) \sim 0$ K] and the second condition is that the initial temperatures are high for both electrons and ions [$T_e(0) = 100$ K, $T_i(0) = 50$ K]. For these two simulations, the number of the ions is 7920 with equivalent number of electrons. The number of particle is chosen to meet the capacity of the computing power we have. The particles are initially placed randomly in a spherical space with a Gaussian distribution,

$$\rho(r) = \rho_0 \exp(-r^2/2\sigma^2), \tag{6}$$

with the width of $\sigma = 1$ μm.

Figure 1(a) shows the temporal evolution of the average kinetic energy of ions with low initial temperature $T_e(0) = 10$ K, $T_i(0) \sim 0$ K, and the peak density $\rho_0 \approx 0.5 \times 10^9$cm^{-3}. $\omega = \sqrt{\rho_0 e^2/m_i\varepsilon_0}$ is the ion kinetic-energy oscillation frequency corresponding to the peak density. In this simulation, the total energy is conserved to an accuracy of $10^{-3}E_0$, where E_0 is the initial total energy of the system. The most characterizing behavior from Fig. 1(a) is the rapid increase in the average kinetic energy of ions by several orders of magnitude, which is the "disorder heating" or "correlation heating." It is due to the fact that the system is created in an uncorrelated condition far from thermodynamic equilibrium. Immediately after the photoionization, the ions created from

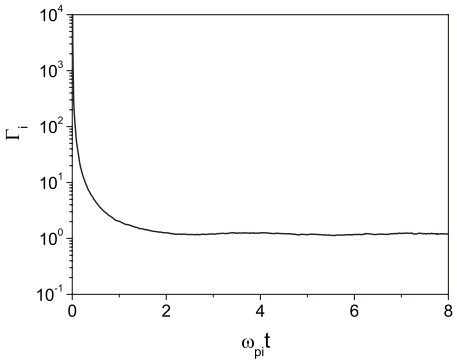

FIG. 2. The ionic Coulomb coupling parameter Γ_i as a function of time. The parameters are the same as in Fig. 1(a).

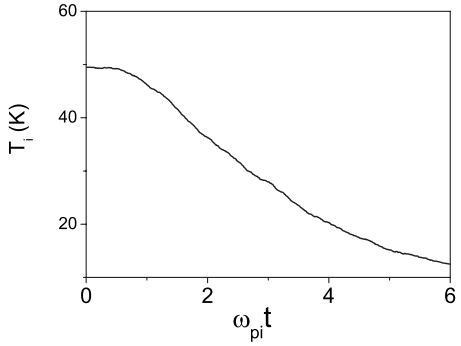

FIG. 3. The time evolution of the average kinetic energy of ions obtained by our simulation with Gaussian initial distribution of the atoms for relatively high initial temperature $T_e(0)=100$ K, $T_i(0)=50$ K, $N_i=N_e=7920$.

an ultracold neutral atomic cloud have very little kinetic energy and they are spatially uncorrelated. During the evolution of the plasma, the ion-ion Coulomb interaction caused the correlation energy to heat the ions, which leads to the increase in ion temperature. As a result the equilibration temperature of ions would be on the order of the Coulomb interaction energy between neighboring ions when photoionization happens [17],

$$k_B T \approx \frac{e^2}{4\pi\varepsilon_0 a}. \tag{7}$$

In our simulation, $T \approx 1.89$ K is estimated from Eq. (7). The potential energy is converted into the kinetic energy leading into $\Gamma \approx 1.2$ as shown in Fig. 2.

The ion kinetic-energy oscillations, which display the universal relaxation dynamics of a strongly coupled Coulomb system, are also reproduced in Fig. 1(a) [16–19]. Other simulation shown in Fig. 1(b) is given for the comparison with our result. Figure 1(b) shows a hybrid molecular dynamics (hybrid-MD) simulation (solid line) compared with experimental data (dots) [17,19]. The initial peak density is $\rho_0(0)=2\times10^9$ cm^{-3} with $N=10^6$ and the initial electron temperature is $T_e(0)=38$ K. In the hybrid-MD simulation [19] only ions are simulated by molecular dynamics method and a mean-field treatment is used for electrons. Comparing with Fig. 1(b), the evolution of the average ion temperature decreases much quicker in this case. This is because of the faster evolution introduced by the mass ratio we used. Although the initial conditions are different, the simulation curve is well matched with the experimental data. It also agrees with the hybrid-MD simulation in reproducing the rapid heating of the plasma and kinetic-energy oscillation.

Figure 3 shows the temporal evolution of the average kinetic energy of ions for a relatively high initial temperature $T_e(0)=100$ K, $T_i(0)=50$ K, and the peak density $\rho_0 \approx 0.5\times10^9$ cm^{-3}. The total energy is conserved to an accuracy of $10^{-5}E_0$. In contrast to Fig. 1(a), the ion kinetic energy reduces quickly as the time increases. The reason why the ion temperature does not rapidly increase as in Fig. 1 is because disorder-induced heating has a small contribution compared with the high initial temperature of ions. The decrease in temperature in Fig. 3 is due to the bulk expansion of the plasma. The high initial temperatures of electrons and ions accelerate the expansion of plasma, resulting in the rapid decrease in the ion temperature.

B. DIH for body-centered-cubic-type lattice initial distribution of atoms

In order to avoid DIH, the ions and electrons are generated from a perfect body-centered-cubic (bcc)-type lattice structure. This can be realized by first obtaining an ultracold atomic gas ensemble and loading it into an optical lattice [12]. With a sufficient trapping potential, the atomic cloud can form a crystal-like ensemble which is also termed as Mott insulator in some literatures. The photoionization light is then applied to the system to create unbound ions and electrons. As this kind of plasma is created from an ordered crystal-like ensemble, in the following discussion, we shall call it an ordered initial distribution compared with the disorder Gaussian initial distribution. The initial state of the plasma corresponds to a spherical volume cut out from a bcc lattice. The temperatures of electrons and ions are 10 K and ~0 K, respectively. The total energy is conserved to an accuracy of $10^{-3}E_0$.

Figure 4(a) shows the temporal evolution of the average kinetic energy of ions with $T_e(0)=10$ K, $T_i(0)\sim0$ K, and the average density $\bar{\rho}\approx7\times10^9$ cm^{-3}. The particle numbers of ions and electrons are $N_e=N_i=3200$. The simulations show that the ion temperature still increases, which is the same as shown in Fig. 1. Because of the ordered initial distribution, the ions are spatially correlated. The initial potential energy is comparable to the potential energy in the equilibrium state. We shall discuss the reason for the heating of ions. In the following part, we shall term the simulation for plasma containing only ions as one-component simulation, and plasma with both electrons and ions as two-component simulation. Figure 4(b) is the temporal evolution of the average kinetic energy for one-component plasma $N_i=30976$ with $T_i(0)\sim0$ K and the average density $\bar{\rho}\approx7\times10^9$ cm^{-3}. The highest temperature that can achieve in Fig. 4(b) is about 110 μK.

By comparing Fig. 4(a) with Fig. 4(b), we conclude that the heating in Fig. 4(a) is due to the collisional heating from

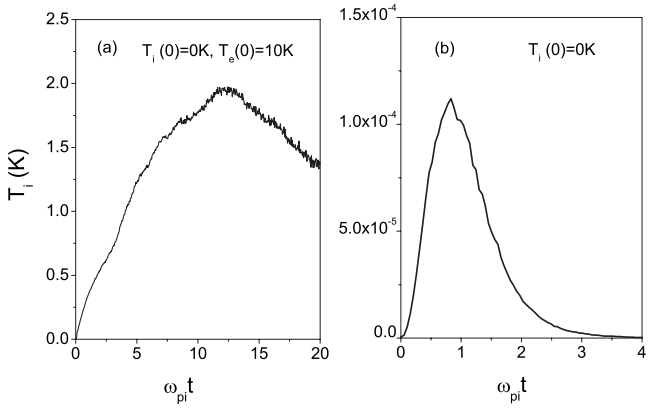

FIG. 4. The time evolution of the average kinetic energy of ions with ordered initial distribution of the atoms: (a) for two-component plasma, $T_e(0)=10$ K, $T_i(0)\sim 0$ K and (b) for one-component (ion) plasma, $T_i(0)\sim 0$ K.

the electrons. The heating rate for ions due to collision with electrons is given by [13,20]

$$\gamma_{heating} = \sqrt{32\pi}\frac{e^4\rho}{\sqrt{m_e k_B T_e}}\frac{m_e}{m_i}\ln\left(\frac{\sqrt{3}}{\Gamma_e^{3/2}}\right). \tag{8}$$

From Eq. (8), one can find that the collisional rate is proportional to the particle density and inversely proportional to $\sqrt{T_e}$. In order to verify the above explanation, we also perform simulations with different densities and initial electron temperatures.

We simulate the two-component plasma with the same condition as used in Fig. 4(a) except $T_e(0)=100$ K in Fig. 5(a). One can find that the highest temperature in Fig. 5(a) is much less than the one in Fig. 4(a). Because the initial electron temperature is high, the collisional heating rate is smaller than that with $T_e(0)=10$ K, which results in the lower temperature in Fig. 5(a). The hot electrons increase the expansion velocity of the ions, which leads to a quick reduction in ion numbers in the given inner region ($0.8R_0$) with the temporal evolution. This is also the reason why the curve in Fig. 5(a) is less smooth than the one in Fig. 4(a). Figure 5(b) shows the numbers of ions in the inner region with radius $R=0.8R_0$ as a function of time for $T_e(0)=100$ K (red dotted line) and $T_e(0)=10$ K (solid line). It is clear that the curve for relatively high initial electron temperature decreases faster.

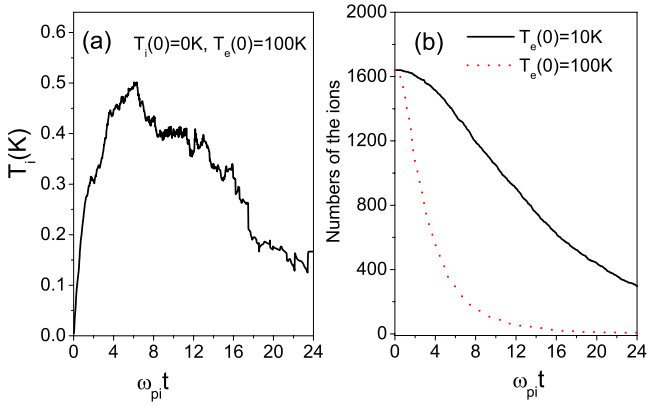

FIG. 5. (Color online) (a) The time evolution of the average kinetic energy of ions with ordered initial distribution of the atoms. The parameters are the same as those in Fig. 4(a), except $T_e(0)=100$ K. (b) The numbers of the ions in the inner region with $0.8R_0$ as a function of time for $T_e(0)=10$ K (solid line) and $T_e(0)=100$ K (red dotted line).

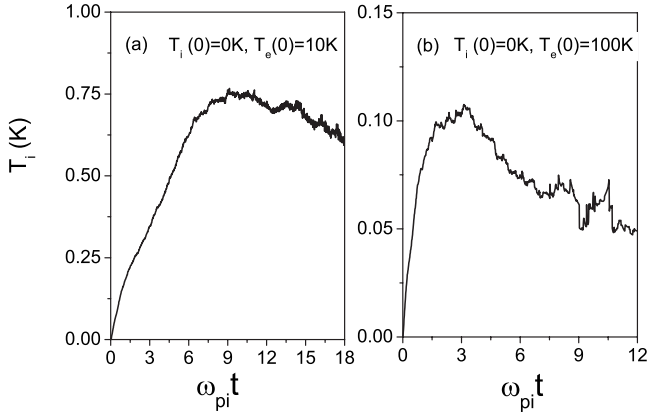

FIG. 6. The time evolution of the average kinetic energy of ions with ordered initial distribution of atoms for low-density two-component plasmas with $N_i=N_e=3584$, (a) $T_e(0)=10$ K, $T_i(0)\sim 0$ K and (b) $T_e(0)=100$ K, $T_i(0)\sim 0$ K.

The collisional rate also depends on the particle density. We further simulate the two-component plasma with lower density $\bar{\rho}\approx 0.8\times 10^9$ cm^{-3}. Figure 6 is the temporal evolution of the average ion kinetic energy for ordered initial distribution plasma with the density $\bar{\rho}\approx 0.8\times 10^9$ cm^{-3} and $T_e(0)=10$ K, $T_i(0)\sim 0$ K [Fig. 6(a)] and $T_e(0)=100$ K, $T_i(0)\sim 0$ K [Fig. 6(b)]. The numbers of ions and electrons are $N_e=N_i=3584$. The highest temperature in Fig. 6(a) is about 0.75 K, which is less than that in Fig. 4(a) with a relatively higher particle density, as expected from Eq. (8). When the initial electron temperature becomes higher, the highest ion temperature in Fig. 6(b) is also less than that with lower electron temperature in Fig. 6(a). The results agree qualitatively well with the collisional heating rate of ions described by Eq. (8). Comparing the heating effect in different initial conditions, we can conclude that the heating effects in Figs. 4(a), 5(a), and 6 result from collisional heating from electrons, not from DIH as shown in Fig. 1.

The ion Coulomb coupling parameter for different initial conditions is shown in Fig. 7, where Fig. 7(a) corresponds to the simulations in Figs. 4(a) and 5(a), and Fig. 7(b) is for Fig. 6. The ion-ion coupling is stronger for a relatively high initial electron temperature and lower ion density. These simulations show that the ion temperature can increase due to the collisional heating from electrons although DIH can be avoided by arranging the ions in a perfect bcc-type lattice structure. In fact, the mass ratio of ion to electron is far greater than 100. The ion heating from electron collision in experiment is much smaller than the simulation results we obtain. If the experimental values of the parameters are carefully prepared, the ion collisional heating from the electrons would be very relatively small and even negligible. In this

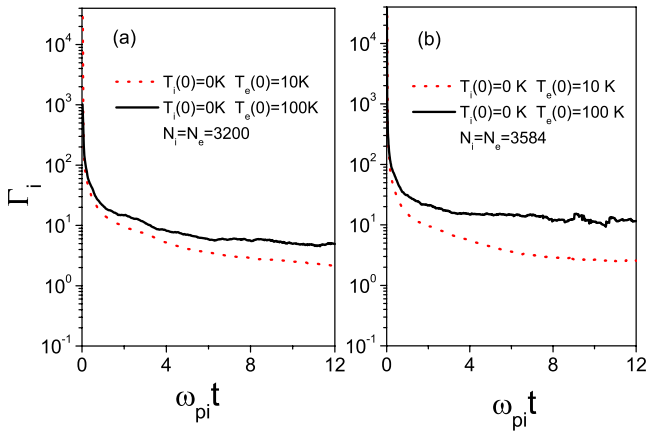

FIG. 7. (Color online) The ion coulomb coupling parameter Γ_i for ordered initial distribution plasmas: (a) for $T_i(0)\sim 0$ K, $T_e(0)=10$ K (red dotted line) and $T_i(0)=0$ K, $T_e(0)=100$ K (solid line). The initial average density is $\bar{\rho}\approx 7\times 10^9$ cm^{-3} and the numbers are $N_i=N_e=3200$, (b) with $T_i(0)\sim 0$ K, $T_e(0)=10$ K (red dotted line) and $T_i(0)\sim 0$ K, $T_e(0)=100$ K (solid line). The initial average density is $\bar{\rho}\approx 0.8\times 10^9$ cm^{-3} and the numbers are $N_i=N_e=3584$.

way we can obtain a strongly coupled ultracold plasma using the perfect bcc-type lattice arrangement as an initial condition.

C. DIH for one-component plasma

Simulations for the bcc-lattice distribution show that the collisional heating from electrons is very important for two-component plasma. Here, we shall see how much the collisional heating contributes to the rapid increase in temperature in Fig. 1(a). In order to do this, we shall simulate the one-component plasmas for different distributions.

In Fig. 8(a), the temporal evolution of the average kinetic energy of ions for one-component plasma is presented, with random Gaussian initial distribution of the atoms and the peak density $\rho_0\approx 0.5\times 10^9$cm^{-3}, $N_i=7920$. The rapid heating of the ions still exists. Comparing the maximal temperature

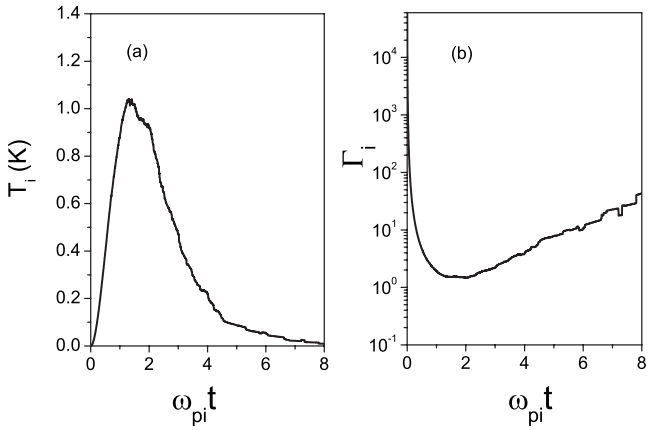

FIG. 8. (a) The time evolution of the average kinetic energy of ions and (b) the ionic coulomb coupling parameter Γ_i as a function of time for one-component plasma with Gaussian initial distribution of the atoms and $T_i\sim 0$ K.

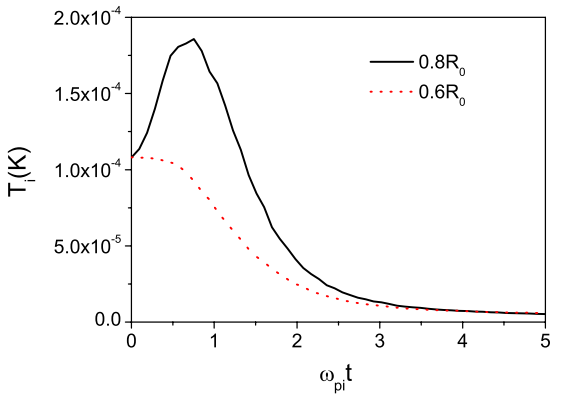

FIG. 9. (Color online) The time evolution of the average kinetic energy of ions with ordered initial distribution of the atoms for two different center regions $0.8R_0$ (solid line) and $0.6R_0$ (red dotted line). The parameters are the same as those in Fig. 4(b).

achieved in Fig. 1(a) with that in Fig. 8(a), we can see that the rapid heating in Fig. 1(a) is due to DIH. The Coulomb coupling parameter is shown in Fig. 8(b). Γ_i decreases quickly to the minimum due to the DIH followed by a slow increase. This is because the ion temperature decreases during the expansion and overcompensates the reduction in the density. In this way the Coulomb coupling parameter increases as the plasma expands.

For one-component plasma with ordered lattice initial distribution, the simulation shown in Fig. 4(b) displays that DIH is absent due to the ordered initial distribution and there is a small temperature increase. In this simulation we define the initial temperature of ions close to 0 K, so the "order-induced cooling" predicted in [8,21] is not clear. In the simulation with the higher initial ion temperature, Fig. 9 shows that the order-induced cooling is observable. In Fig. 9, $T_i(t)$ is compared for regions with radii of $0.8R_0$ (solid line) and $0.6R_0$ (red dotted line). The temperature increases in the $0.8R_0$ region at the beginning. In contrast, the temperature in the $0.6R_0$ region reduces with time increasing. The temperature difference between the two regions is due to the edge effect resulting in an imperfect correlated system. When we analyze the system with an open boundary, this edge effect is observed in the simulation. If we only consider the inner region ($0.6R_0$), the order-induced cooling appears, as shown in Fig. 9, because the edge effect is negligible for the center region. The temperature increases for one-component plasma with ordered initial distributions resulting from the edge effect of the system.

IV. CONCLUSION

In conclusion, we use molecular dynamics method to simulate the dynamics of the ultracold plasma for different initial conditions. For random Gaussian initial distribution of the particles, the temporal evolution of the average ion kinetic energy displays disorder-induced heating. The oscillation of the kinetic energy is also observed when the initial temperatures of particles are relatively low. These characteristics are qualitatively consistent with experimental data and

other simulations methods. Furthermore, when the initial temperatures are high, the kinetic energy of ions shows approximately Gaussian structures as time increases, which also agrees with the relations for high initial temperature of electrons [17]. However, for ordered initial distribution of the particles, the ions can also be heated although DIH is absent. We demonstrate that the main reason of this heating is due to the collisions with electrons. When the plasma density decreases, the rate of collisional heating of ions reduces and the highest ion temperature achieved in the process of the plasma expansion becomes smaller. It is more interesting that relatively high initial temperature of electrons also contributes to stronger coupling between ions. Experimentally if the values of the parameters are appropriate, the collisional heating for the ions would be very small, and the ion-ion strong coupling is possible for the ordered initial distribution in a lattice structure. Finally, we also simulate plasma containing only ions. For random Gaussian initial distribution, the results show that the rapid temperature increase is mainly caused by the disorder-induced heating. With an ordered lattice initial distribution, the order-induced cooling is also observed.

ACKNOWLEDGMENTS

The authors thank Dr. Zhao Yuan Ma for discussions. This project was supported by the National Science Foundation of China under Grant No. 10705042 and Shanghai Supercomputer Center of China.

[1] T. C. Killian, S. Kulin, S. D. Bergeson, L. A. Orozco, C. Orzel, and S. L. Rolston, Phys. Rev. Lett. **83**, 4776 (1999).
[2] S. Kulin, T. C. Killian, S. D. Bergeson, and S. L. Rolston, Phys. Rev. Lett. **85**, 318 (2000).
[3] T. C. Killian, M. J. Lim, S. Kulin, R. Dumke, S. D. Bergeson, and S. L. Rolston, Phys. Rev. Lett. **86**, 3759 (2001).
[4] M. P. Robinson, B. Laburthe Tolra, M. W. Noel, T. F. Gallagher, and P. Pillet, Phys. Rev. Lett. **85**, 4466 (2000).
[5] E. Eyler, A. Estrin, R. Ensher, C. H. Cheng, C. Sanborn, and P. L. Gould, Bull. Am. Phys. Soc. **45**, 56 (2000).
[6] S. Ichimaru, Rev. Mod. Phys. **54**, 1017 (1982).
[7] D. H. E. Dubin and T. M. O'Neil, Rev. Mod. Phys. **71**, 87 (1999).
[8] D. O. Gericke and M. S. Murillo, Contrib. Plasma Phys. **43**, 298 (2003).
[9] J. L. Roberts, C. D. Fertig, M. J. Lim, and S. L. Rolston, Phys. Rev. Lett. **92**, 253003 (2004).
[10] M. S. Murillo, Phys. Rev. Lett. **87**, 115003 (2001).
[11] T. Pohl, T. Pattard, and J. M. Rost, Phys. Rev. Lett. **92**, 155003 (2004).
[12] T. Pohl, T. Pattard, and J. M. Rost, J. Phys. B **37**, L183 (2004).
[13] S. G. Kuzmin and T. M. O'Neil, Phys. Plasmas **9**, 3743 (2002).
[14] S. Mazevet, L. A. Collins, and J. D. Kress, Phys. Rev. Lett. **88**, 055001 (2002).
[15] M. S. Murillo and M. W. C. Dharma-wardana, Phys. Rev. Lett. **100**, 205005 (2008).
[16] M. S. Murillo, Phys. Rev. Lett. **96**, 165001 (2006).
[17] T. C. Killian, T. Pattard, T. Pohl, and J. M. Rost, Phys. Rep. **449**, 77 (2007).
[18] T. C. Killian, Science **316**, 705 (2007).
[19] T. Pohl, T. Pattard, and J. M. Rost, Phys. Rev. Lett. **94**, 205003 (2005).
[20] D. V. Sivukhin, *Reviews of Plasma Physics* (Consultants Bureau, New York, 1966), Vol. 4, p. 138.
[21] M. S. Murillo, Phys. Plasmas **14**, 055702 (2007).